CUTL1 is a target of TGFβ signaling that enhances cancer cell motility and invasiveness

Patrick Michl,[1,6] Antoine R. Ramjaun,[1] Olivier E. Pardo,[1] Patricia H. Warne,[1] Martin Wagner,[3] Richard Poulsom,[2] Corrado D'Arrigo,[4] Kenneth Ryder,[5] Andre Menke,[3] Thomas Gress,[3] and Julian Downward[1,*]

[1]Signal Transduction Laboratory, Cancer Research UK London Research Institute, 44 Lincoln's Inn Fields, London WC2A 3PX, United Kingdom
[2]In Situ Hybridisation Service, Cancer Research UK London Research Institute, 44 Lincoln's Inn Fields, London WC2A 3PX, United Kingdom
[3]Abteilung Innere Medizin I, Klinikum der Universität Ulm, Robert-Koch-Strasse 8, 89081 Ulm, Germany
[4]Cancer Research UK Breast Cancer Pathology Laboratory, Guy's Hospital, St. Thomas Street, London SE1 9RT, United Kingdom
[5]Clinical Oncology Unit, Guy's Hospital, St. Thomas Street, London SE1 9RT, United Kingdom
[6]Present address: Abteilung Innere Medizin I, Klinikum der Universität Ulm, Robert-Koch-Strasse 8, 89081 Ulm, Germany
*Correspondence: julian.downward@cancer.org.uk

Summary

CUTL1, also known as CDP, Cut, or Cux-1, is a homeodomain transcriptional regulator known to be involved in development and cell cycle progression. Here we report that CUTL1 activity is associated with increased migration and invasiveness in numerous tumor cell lines, both in vitro and in vivo. Furthermore, we identify CUTL1 as a transcriptional target of transforming growth factor β and a mediator of its promigratory effects. CUTL1 activates a transcriptional program regulating genes involved in cell motility, invasion, and extracellular matrix composition. CUTL1 expression is significantly increased in high-grade carcinomas and is inversely correlated with survival in breast cancer. This suggests that CUTL1 plays a central role in coordinating a gene expression program associated with cell motility and tumor progression.

Introduction

CUTL1, also known as CDP (CCAAT displacement protein), Cut, or Cux-1, belongs to a family of homeobox transcription factors involved in the regulation of cell growth and differentiation (Nepveu, 2001). It is evolutionarily conserved and contains four DNA binding domains, three of which are known as Cut repeats and one as a Cut homeodomain (Harada et al., 1995).

CUTL1 has been described as a transcriptional activator as well as a transcriptional repressor. Its activity has been associated with cellular proliferation and cell cycle progression (Van Wijnen et al., 1996; Coqueret et al., 1998; Truscott et al., 2003), as well as modulation of genes involved in terminal differentiation (van Gurp et al., 1999; Skalnik et al., 1991). Knockout studies with the murine homolog, Cux-1, revealed reduced growth, retarded differentiation of the lung epithelia, hair follicle defects, reduced male fertility, and deficient T and B cell function (Ellis et al., 2001; Luong et al., 2002; Sinclair et al., 2001). In contrast, mice transgenic for Cux-1 showed organomegaly and multiorgan hyperplasia (Ledford et al., 2002).

CUTL1 has been demonstrated to be a phosphorylation target of several kinases that modulate its DNA binding affinity: phosphorylations by cyclin A-cdk1 and by PKC at various sites have been shown to inhibit DNA binding activity (Coqueret et al., 1996; Santaguida et al., 2001). No reports exist so far on the transcriptional regulation of CUTL1 in mammalian cells. Studies in flies indicate that the *Drosophila* homolog of CUTL1, Cut, is a major determinant of cell type specification downstream of the notch pathway (Tavares et al., 2000) and may also interact with the wingless (Wg) signaling pathway (Micchelli et al., 1997).

The role of CUTL1 in tumorigenesis and tumor progression remains to be elucidated. Although initial databases on loss of heterozygosity studies suggested that CUTL1 might be a candidate tumor suppressor gene (Zeng et al., 1999), a recent report suggests instead that CUTL1 could play a role in promoting breast cancer: Goulet et al. describe a tissue-specific CUTL1 isoform that appears to be strongly expressed in some breast tumors and, when overexpressed, inhibits tubule formation of breast cancer cells in vitro (Goulet et al., 2002).

SIGNIFICANCE

The ability to migrate and invade into surrounding tissues, blood, and lymphatic vessels is one of the hallmarks of cancer and a prerequisite for local tumor progression and metastatic spread. However, the underlying mechanisms controlling cell invasiveness remain poorly understood. TGFβ is known as one of the key factors modulating cell migration, invasion, and tumor progression. In this study, we identify CUTL1, a transcription factor involved in development and cell differentiation, as a major regulator of cell motility and invasion and an important downstream effector of TGFβ. The fact that CUTL1 expression is increased in high-grade carcinomas and inversely correlated with survival in breast cancer underlines its important role in tumor progression.

Numerous signaling pathways have been implicated in the regulation of tumor progression and cell invasion. TGFβ is known to be a major modulator of tumor cell migration (Massague, 1998), invasiveness (Seton-Rogers et al., 2004), and epithelial-mesenchymal transition (EMT) (Grunert et al., 2003). In addition to the canonical Smad-mediated signaling pathway, TGFβ also activates other pathways involving mitogen-activated protein kinases (MAPK), including JNKs and p38MAPK (Yu et al., 2002).

We have identified CUTL1 in a high-throughput screen for modulators of cell motility using an RNA interference library-based approach (O.E.P. and J.D., unpublished data). In this assay, CUTL1 was discovered as a potential positive regulator of cell motility. Based on these results, we aimed to characterize the role of CUTL1 in the control of cell migration, invasiveness, and tumor progression. Here we demonstrate that CUTL1 strongly promotes cell motility and invasiveness in a variety of cell systems in vitro and in vivo. In addition, we investigated the effects of tumor-related signaling pathways on the transcriptional activity of CUTL1. We could show that CUTL1 is a transcriptional target of TGFβ, thereby mediating promigratory effects of TGFβ. The important role of CUTL1 in promoting cell motility and invasiveness is underlined by the fact that CUTL1 expression is strongly associated with a less differentiated phenotype in breast and pancreatic carcinomas and with decreased patient survival in invasive breast cancer.

Results

Generation of cell lines stably expressing CUTL1 RNAi vector

CUTL1 was identified in a high throughput RNA interference screen for genes that influence cell motility. This screen utilized the Netherlands Cancer Institute RNA interference library, which targets 8,000 human genes (Berns et al., 2004), and will be described in detail elsewhere (O.E.P. and J.D., unpublished data). Briefly, three RNA interference vectors against each gene were cotransfected together with a GFP expression construct into highly motile carcinoma cells. One gene was analyzed per transfected well. After two days, fluorescent cells were identified and tracked by time-lapse video microscopy for a further day. Cells expressing CUTL1 RNAi vectors showed significantly decreased motility.

In order to study the biological role of endogenous CUTL1, we stably suppressed CUTL1 expression by vector-based transfection of specific short hairpin RNA (shRNA) in NIH3T3 fibroblasts, which express high endogenous CUTL1 levels and are known to be highly motile. A number of clones that showed no detectable CUTL1 expression (Figure 1A) were used for further studies. Expression differences of nuclear CUTL1 could also be confirmed by immunocytochemistry (Figure 1B). Interestingly, diminished CUTL1 expression was associated with a strikingly altered cell morphology. CUTL1 RNAi clones were increased in cell size and appeared to be less spindle-shaped compared to control clones a with normal fibroblast-like phenotype (Figure 1C). The increase in cell size was confirmed by various FACS-based assays, including forward scatter, fluorescein diacetate staining, and FITC staining (data not shown).

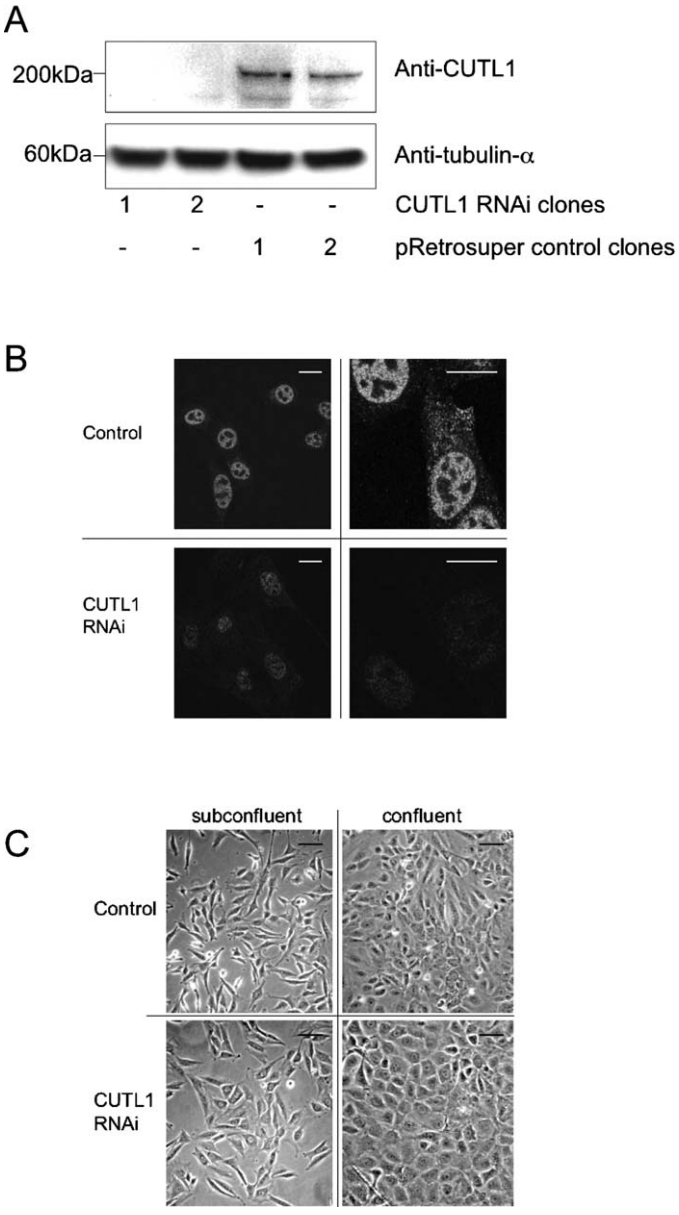

Figure 1. Generation of NIH3T3 cell lines stably expressing CUTL1 RNAi

A: Western blot with anti-CDP (Santa Cruz) showing two representative NIH3T3 clones stably transfected with shRNA for mCUTL1 as compared to control (empty vector only) cells.

B: Immunocytochemical detection of nuclear CUTL1 in NIH3T3 control and CUTL1 RNAi cells, as determined by immunostaining with anti-CDP (Santa Cruz). Bars represent 10 μm.

C: Morphological appearance of subconfluent and confluent NIH3T3 control and CUTL1 shRNA cells, as shown by phase-contrast microscopy. Bars represent 50 μm.

CUTL1 enhances migration and invasion

To examine the effects of CUTL1 on cell motility and migration, we employed three different tissue culture assays examining various aspects of migratory behavior. First, directed migration into an artificial "wound" was measured in a confluent monolayer culture of NIH3T3 cells with or without endogenous CUTL1 expression (control versus CUTL1 RNAi). Control cells extensively migrated into the wound area within 8 hr, but this was significantly reduced in CUTL1 RNAi cells (Figures 2A and 2B). Similar results were also obtained by using two-chamber

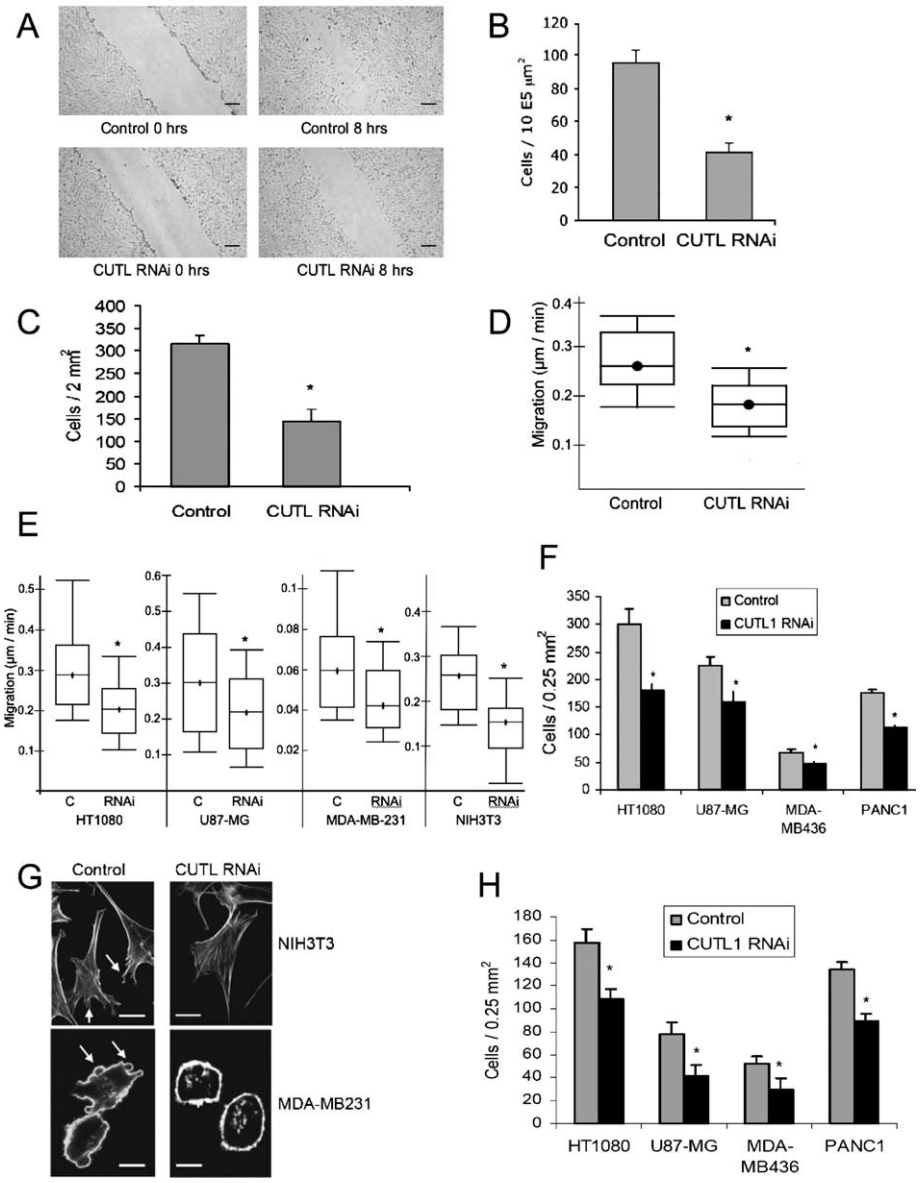

Figure 2. CUTL1 enhances migration and invasion

A: Wound healing assay with NIH3T3 control and CUTL1 RNAi cells. Bar represent 200 μm.

B: Quantification of cells migrated into a defined wound area after 8 hr. Cells in 4 defined areas per group per experiment were quantified. Data are representative for three independent experiments and are shown as mean ± SEM. *p < 0.05 as compared to control cells.

C: Quantification of the two-chamber migration assay of NIH3T3 control and stable CUTL1 shRNA cells. Fixed and stained cells on the bottom side of an 8 μm pore membrane were counted as migrated cells/2 mm^2. Data are representative for three independent experiments and are shown as mean ± SEM. *p < 0.05 as compared to control cells.

D: Video time-lapse microscopy of NIH3T3 control and stable CUTL1 shRNA cells. At least 48 cells per condition per experiment were tracked. Data are presented as bar and whisker graphs, showing the median and the distribution of 50% (bar) and 90% (whisker) of all tracked cells, and are representative of three independent experiments. *p < 0.05 as compared to control cells.

E: Video time-lapse microscopy of HT1080, U87-MG, MDA-MB-231, and NIH3T3 cells with (RNAi) or without (C) transient suppression of CUTL1 by siRNA (oligonucleotides hCUTL1/I for human cells or mCUTL1 for NIH3T3 cells). Data are presented as bar and whisker graphs, and are representative of three independent experiments. *p < 0.05 as compared to control cells.

F: Quantification of two-chamber migration assay with HT080, U87-MG, MDA-MB-436, and PANC1 cells transiently transfected with control and CUTL1 siRNA (oligonucleotide hCUTL1/I). Fixed and stained cells on the bottom side of an 8 μm pore membrane were counted as migrated cells/2 mm^2. Data are representative for three independent experiments and are shown as mean ± SEM. *p < 0.05 as compared to control cells.

G: Representative phalloidin staining for actin cytoskeleton in NIH3T3 cells stably transfected with CUTL1 shRNA and MDA-MB-231 cells with or without transient suppression of CUTL1 by siRNA (oligonucleotide hCUTL1/I). Sites of adhesion sites are indicated by arrows. Bars represent 10 μm.

H: Two-chamber invasion assay of HT1080, U87-MG, MDA-MB-436, and PANC1 cells with or without transient suppression of CUTL1 by siRNA (oligonucleotide hCUTL1/I). Invaded cells in 4 fields per group were counted. Data are representative of three independent experiments. *p < 0.05 as compared to control cells.

migration assays in which cells migrated through a membrane with 8 μm pores from serum-free medium toward 10% FCS-containing medium. In the CUTL1 RNAi clones, the proportion of migrated cells was significantly reduced (Figure 2C).

Knockdown of CUTL1 also slightly reduced cell proliferation, but to a much lesser extent than its effects on migration (see Supplemental Figure S1). To rule out a bias due to differences in proliferation, we also tracked single cells by video time-lapse microscopy, whereby we could confirm that CUTL1 RNAi cells displayed significantly lower motility (Figure 2D). For representative time-lapse video, see Supplemental Videos.

To demonstrate that these observations are not specific for fibroblasts or for a single CUTL1 RNA interference sequence, we performed video time-lapse microscopy and two-chamber migration assays on a variety of different cell lines after transient transfection of synthetic siRNA oligonucleotides targeting different regions of CUTL1 to the shRNA vector. First, we could demonstrate that with this transient approach, we could achieve a marked reduction of CUTL1 protein levels in all cell lines used (see Supplemental Figure S2). Various cell lines of different origin, such as fibrosarcoma (HT1080), glioblastoma (U87-MG), and breast cancer (MDA-MB-231) cells all showed significantly reduced motility when endogenous CUTL1 was suppressed, as assayed by time-lapse microscopy (Figure 2E). This was also confirmed by two-chamber migration assays for a variety of cell lines of mesenchymal and epithelial origin, in-

cluding PANC1 pancreatic carcinoma cells (Figure 2F). To demonstrate that the observed effect was not an off-target effect of one particular siRNA oligonucleotide, we confirmed that two different oligonucleotides targeting different regions of the CUTL1 mRNA were able to decrease CUTL1 expression paralleled by a decreased migration in HT1080 cells (see Supplemental Figure S3). Furthermore, the suppression of CUTL1 led to a marked actin reorganization and a decrease in focal adhesions and membrane protrusions associated with cell motility, as assayed by phalloidin staining, in both NIH3T3 fibroblasts and MDA-MB-231 epithelial cells (Figure 2G and Supplemental Figure S4). The decreased number of focal adhesions in NIH3T3 cells was confirmed by a decrease in vinculin-positive adhesion sites (see Supplemental Figure S5).

To examine whether CUTL1 also affects invasiveness involving movement through a three-dimensional matrix, we performed in vitro invasion assays with several invasive cell lines, including MDA-MB-231 breast cancer and PANC1 pancreatic cancer cells. Invasion through a membrane with 8 μm pores coated with a 30 μm layer of Matrigel consisting of extracellular matrix proteins was significantly reduced by over 30% in either cell line when endogenous CUTL1 was transiently suppressed by siRNA transfection (Figure 2H).

To confirm these results implicating CUTL1 in invasiveness in vivo, we generated stable CUTL1 knockdown clones by shRNA vector introduction into the invasive cell lines HT1080 fibrosarcoma, MDA-MB-436 breast carcinoma, and PANC1 pancreatic carcinoma, resulting in a significant reduction of CUTL1 expression in each cell line (Figures 3A and 3B and data not shown). Tail vein injection of two clones each with or without endogenous CUTL1 knockdown into nude mice resulted in a significant reduction of pulmonary metastatic colonizations, both in number and size (Figures 3C–3E and data not shown). It is therefore likely that CUTL1 expression may be important in establishing a transcriptional program that is conducive to metastatic behavior of cells in vivo.

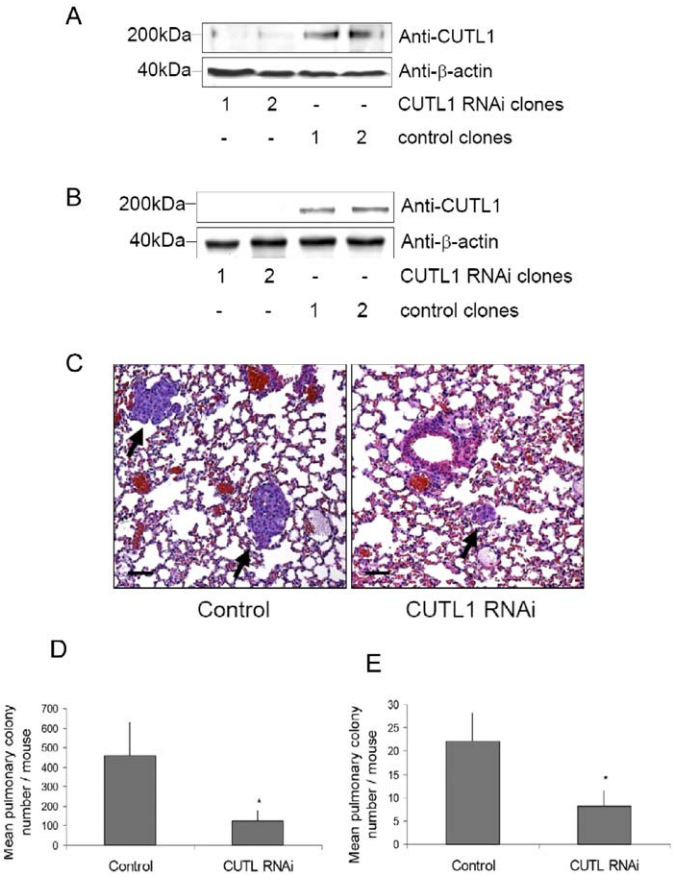

Figure 3. CUTL1 enhances pulmonary colonization in vivo

A: Western blot with anti-GST-CUTL1 showing two representative HT1080 clones each stably transfected with shRNA for hCUTL1 as compared to control (empty vector only) cells.

B: Western blot with anti-GST-CUTL1 showing two representative MDA-MB-436 clones each stably transfected with shRNA for hCUTL1 as compared to control (empty vector only) cells.

C: Representative H&E staining for pulmonary colonizations with HT1080 control and CUTL RNAi cells 17 days after tail vein injections into nu/nu mice. Pulmonary colonies are marked with an arrow. Bars represent 100 μm.

D: Quantification of the pulmonary colonizations with stable HT1080 control and CUTL1 shRNA cells 17 days after tail vein injection into nu/nu mice. Data are presented as mean number of colonies per animal, as assayed in serial H&E sections of the lungs (15 sections at a distance of 150 μm from each other), and are representative for 2 CUTL1 RNAi clones and 2 control clones each. *p = 0.05 as compared to control cells. Data shown are mean ± SEM.

E: Quantification of the pulmonary colonizations with stable MDA-MB-436 control and CUTL1 shRNA cells 40 days after tail vein injection into nu/nu mice. Data are presented as mean number of colonies per animal, as assayed in serial H&E sections of the lungs (15 sections at a distance of 150 μm from each other), and are representative for 2 CUTL1 RNAi clones and 2 control clones each. *p = 0.05 as compared to control cells. Data shown are mean ± SEM.

CUTL1 is transcriptionally upregulated by TGFβ

Given the major role of TGFβ in regulating migration and invasiveness, we were interested in whether TGFβ influences CUTL1 activity. We found that CUTL1 is transcriptionally upregulated by TGFβ in numerous cell lines such as NIH3T3 fibroblasts, AML12 hepatocytes, HT1080 fibrosarcoma, MDA-MB-231 and MDA-MB-436 breast cancer, HCT116 colon cancer, and PANC1 pancreatic cancer cells (Figures 4A and 4D and data not shown). This TGFβ effect was mediated via TGFβRI, since SB431542, an inhibitor of ALK4/5/7 (Inman et al., 2002), was able to abolish TGFβ-induced upregulation of CUTL1, as confirmed in NIH3T3 cells (Figure 4B), MDA-MB-231 cells, and PANC1 cells (data not shown). A weaker induction of CUTL1 expression on serum treatment was not SB431542-sensitive, suggesting that TGFβ-independent pathways also affect CUTL1 transcription. CUTL1 mRNA induction by TGFβ appeared 4 hr after addition of TGFβ, suggesting that CUTL1 is not one of the early response genes of TGFβ (Figure 4C). To investigate the pathways acting downstream of TGFβ in CUTL1 upregulation, we used clones of the mouse hepatocyte cell line AML12 in which the expression of Smad4 had been stably suppressed by shRNA (A.R.R. and J.D., unpublished data) as well as MDA-MB-436 breast cancer cells with or without transient suppression of Smad4 by siRNA. AML12 cells lacking Smad4 showed significantly lower CUTL1 protein levels than wild-type cells (Figure 4D), as did MDA-MB-436 cells with transient Smad4 suppression (see Supplemental Figure S6) and PANC1 cells (data not shown), indicating that Smad4-dependent signaling is involved in the transcriptional regulation of CUTL1. In addition, coincubation with the

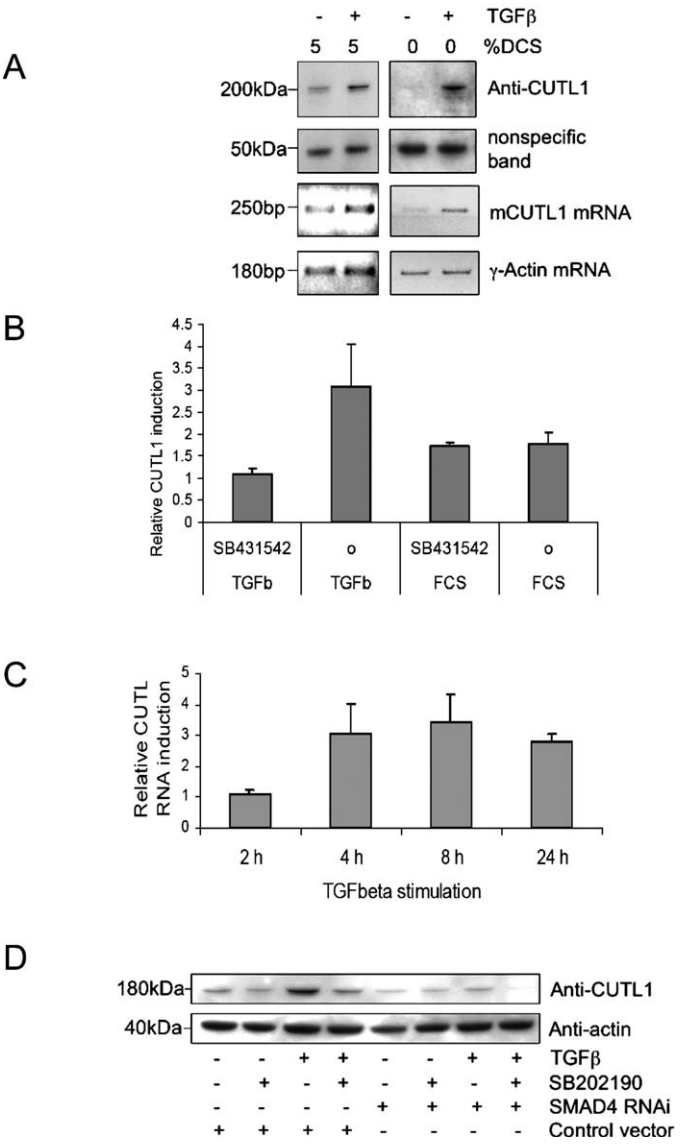

Figure 4. TGFβ induces CUTL1 expression via Smad4 and p38MAPK

A: TGFβ increases CUTL1 expression at mRNA (4 hr) and protein level (10 hr) in NIH3T3 cells grown in the presence or absence of serum. RT-PCR was performed using mCUTL1 specific primers, and Western blot was performed with rabbit anti-CDP antibody (Santa Cruz).

B: The TGFβ receptor type I inhibitor SB431542 decreases TGFβ-induced CUTL1 induction, as assessed by real-time PCR. NIH3T3 cells preincubated with or without SB431542 (10 μM) for 30 min were stimulated with TGFβ (10 ng/ml) under serum-free conditions or with 10% FCS for additional 4 hr. Data are shown as CUTL1 mRNA expression relative to unstimulated control and are representative for three independent experiments. Data shown are mean ± SEM.

C: Time course of TGFβ-induced CUTL1 expression under serum-free conditions, as assessed by real-time PCR. Data are shown as CUTL1 expression relative to unstimulated control and are representative for three independent experiments. Data shown are mean ± SEM.

D: Western blot of CUTL1 transcriptional regulation by TGFβ and p38MAPK inhibitor SB202190 in AML12 hepatocytes with or without stable suppression of SMAD4 by shRNA. Anti-CDP antibody (Santa Cruz) was used. Cells were grown in 10% fetal calf serum.

p38MAPK inhibitor SB202190 resulted in additional downregulation of both basal and TGFβ-induced CUTL1 levels (Figure 4D and Supplemental Figure S6), indicating that p38MAPK-dependent signaling, known to be an additional effector pathway downstream of TGFβ, also plays a role in modulating CUTL1 levels.

CUTL1 is required for TGFβ effects on migration

To test the biological significance of the TGFβ-induced upregulation of CUTL1, we examined the influence of CUTL1 on migration in the presence or absence of TGFβ. Addition of TGFβ significantly increased the migration of NIH3T3 control cells, paralleled by an increase in CUTL1 levels. In contrast, in stable CUTL1 RNAi NIH 3T3 cells, the effect of TGFβ on the basal migration rate was absent (Figure 5A). These results were confirmed by two-chamber migration assays (Figure 5B) and wound healing assays (Figure 5C). Furthermore, transient transfection of HT1080 fibrosarcoma cells with CUTL1 siRNA confirmed that both basal and TGFβ-induced migration strongly correlate with the level of CUTL1 expression (Figure 5D), which was also observed in MDA-MB-231 breast cancer cells (data not shown). Based on these data, it appears likely that CUTL1 expression is required for TGFβ to exert its promigratory effects. To examine whether CUTL1 mediates TGFβ-induced epithelial-mesenchymal transition (EMT), thereby enhancing cell migration, we used EpH4 and Ha-Ras-transformed EpH4 (EpRas) mammary epithelial cells before and after TGFβ-induced EMT (EpRasXT cells), a cell system which has been described as a model system for EMT (Jechlinger et al., 2003). However, despite decreasing cell motility as confirmed by Boyden chamber assays, CUTL1 knockdown did not in any way alter the expression levels of any of the marker proteins associated with EMT, such as E cadherin, vimentin, or cytokeratin 8/18 (data not shown). Therefore, CUTL1 seems to mediate promigratory effects of TGFβ independently of EMT and does not appear to play a role in the regulation of EMT.

Transcriptional effects of CUTL1 knockdown

To determine the transcriptional program regulated by CUTL1 that might underlie the differences seen in cell motility and invasion, we performed Affymetrix microarray gene expression profiling experiments with two NIH3T3 CUTL1 RNAi clones and two control clones.

Using highly stringent significance criteria, we generated lists containing genes which were more highly expressed in control relative to CUTL1 RNAi cells (Table 1, Upregulated by CUTL1) or more highly expressed in CUTL1 RNAi relative to control cells (Table 2, Downregulated by CUTL1). The genes were grouped into several categories by their ontological classification using the MAPPFinder software and the available literature.

The group of upregulated genes mainly consists of genes related to embryonic development and differentiation, genes involved in adhesion and cell motility, genes encoding secreted extracellular matrix proteins, and genes encoding various transcription factors and enhancers of protein synthesis (Table 1). Many of these have previously been described as modulators of cell invasion in various tumor cell models (see Discussion). The group of downregulated genes (Table 2) consists mainly of genes associated with inflammatory reaction, acute-phase response, and chemotaxis, as well as genes encoding secreted

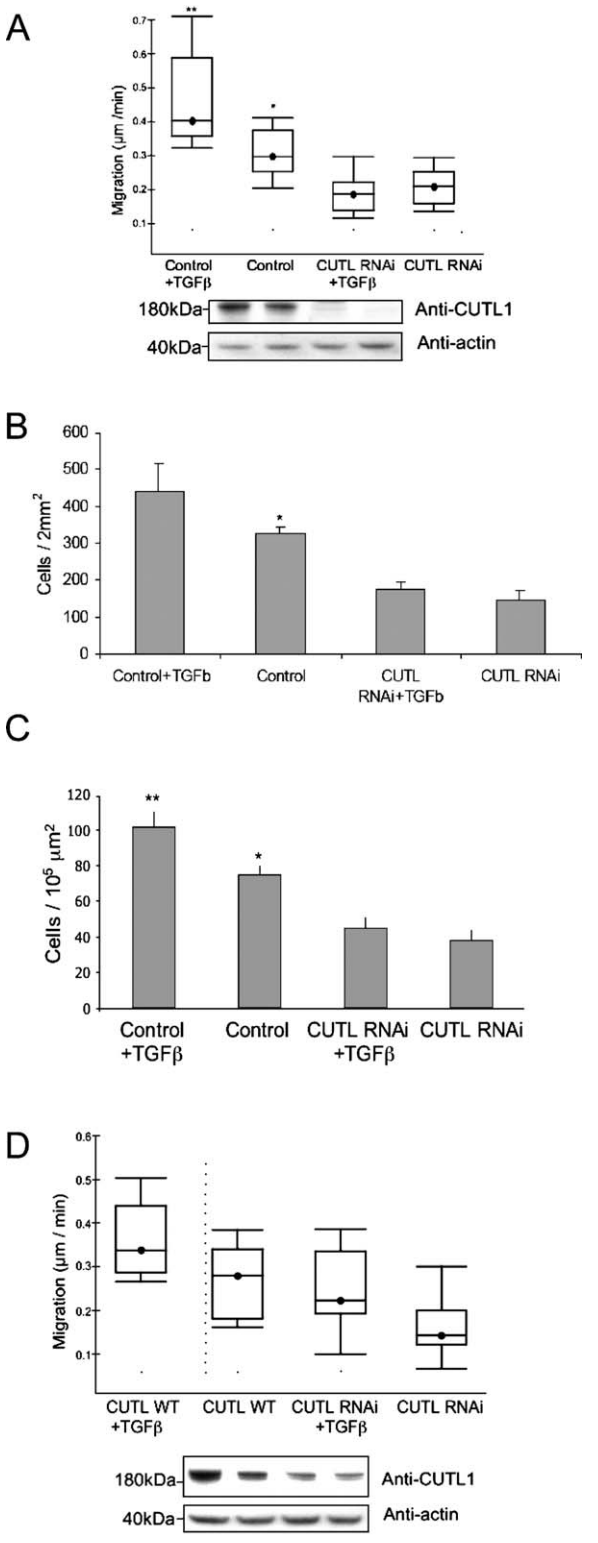

Figure 5. CUTL1 mediates TGFβ effects on migration and invasion

A: Video time-lapse microscopy of NIH3T3 control and stable CUTL1 shRNA cells ± TGFβ. Data are presented as bar and whisker graphs and are representative of three independent experiments. *p < 0.05 as compared to CUTL1 shRNA cells. **p < 0.05 as compared to control cells. In parallel, CUTL1 expression in cells under each condition was determined by Western blot (lower panel). 10% donor calf serum containing medium was used.

B: Quantification of the two-chamber migration assay of stable NIH3T3 control and CUTL1 shRNA cells ± TGFβ. Fixed and stained cells on the bottom side of the membrane were counted and quantified as migrated cells/2 mm^2. Data are representative for three independent experiments and are shown as mean ± SEM. *p < 0.05 as compared to CUTL RNAi cells.

C: Wound healing assay with stable NIH3T3 control and CUTL1 shRNA cells ± TGFβ. Cells in 4 defined areas per group per experiment were quantified. Data are representative for three independent experiments and are shown as mean ± SEM. *: p < 0.05 as compared to CUTL1 RNAi cells. **: p < 0.05 as compared to control cells.

D: Video time-lapse microscopy of HT1080 cells with or without transiently suppressed CUTL1 by siRNA (oligonucleotide hCUTL1/I) ± TGFβ. Data are representative of three independent experiments. Simultaneously, cells were treated identically and harvested for Western blot in order to analyze CUTL1 expression (lower panel). Experiments were performed in serum containing medium.

extracellular matrix proteins. We could confirm the microarray data for the vast majority of the genes tested, both on RNA (see Supplemental Figure S7) and protein levels (see Supplemental Figure S8) as well as on promoter level for selected genes (see Supplemental Figure S9). To demonstrate that the identified target genes are not specific for NIH3T3, we performed additional experiments using real-time PCR after transient knockdown of CUTL1 in various cancer cell lines. We could confirm that several CUTL1 target genes identified by the microarray experiments, such as WNT5A, were also regulated by CUTL1 in fibrosarcoma and breast and pancreatic cancer cells (see Supplemental Figure S10).

Taken together, these microarray results suggest that CUTL1 predominantly regulates genes involved in migration, invasion, adhesion, and modulation of the extracellular matrix, indicating that it might be involved in the control of cell motility in vitro and invasiveness in tumors.

CUTL1 expression is increased in high-grade breast and pancreatic cancers

As reduction in CUTL1 expression leads to reduced motility and invasiveness of cell lines from several tissue origins both in vitro and in vivo, we sought to elucidate the physiological relevance of CUTL1 in tumor progression and metastasis by studying CUTL1 expression in 138 patients with invasive ductal carcinoma of the breast where full histopathological data and active clinical followup up to 22 years were available. This cohort was analyzed for known prognostic markers (estrogen receptor, progesterone receptor, tumor size, lymph node status, histological grade) and showed trends in overall and relapse-free survival in keeping with the expected outcome. For detailed patient characteristics, see Supplemental Table S1. In situ hybridization on multiple tissue core arrays showed CUTL1 expression in more than half of the tumors. Interestingly, poorly differentiated high-grade (G3) breast carcinomas expressed significantly more CUTL1 than well-differentiated low-grade (G1) tumors (Figures 6A and 6B). This correlation was confirmed in an independent series of 35 breast cancer tissues by immunohistochemistry, demonstrating higher expression of CUTL1 protein in G2 and G3 tumors as compared to G1 tumors (Figures 6C and 6D). Furthermore, in patients with high-grade (G3) tumors, CUTL1 expression, as assessed by ISH, inversely correlated with relapse-free survival (Figure 6E) and overall survival (see Supplemental Figure S11) as a prognostic marker. To further corroborate our data with another epithelial

Table 1. Genes upregulated by CUTL1

Annotation	Ratio CUTL/RNAi	Gene symbol	Full name
Development/differentiation			
Mm.103593	49.7	DKK2	dickkopf-2
Mm.3063	8.1	PTN	pleiotrophin
Mm.8180	3.9	DPYSL3	dihydropyrimidinase-LIKE 3
Mm.32207	2.4	WNT5A	wingless-type mmtv integration site, member 5a
Mm.29205	2.3	BRUNOL4	bruno-like 4
Mm.89924	2.1	MRPPLF3	mitogen-regulated protein proliferin-3
Mm.139314	2.1	DPPA5	developmental pluripotency associated-5
Mm.9336	2.1	GNB4	guanine nucleotide-binding protein, beta-4 subunit
Adhesion/motility			
Mm.29798	5.0	CD34	hematopoietic progenitor cell antigen cd34
Mm.2877	4.7	ALCAM	activated leukocyte cell adhesion molecule
Mm.225096	3.3	ITGA6	integrin, alpha-6
Mm.16749	2.9	KLRA18	killer cell lectin-like receptor a18
Mm.154610	2.7	TM4SF10	transmembrane 4 superfamily, member10
Mm.1	2.0	S100A10	100 calcium binding protein a10 (calpactin)
Extracellular matrix			
Mm.25755	3.5	ASPN	asporin
Mm.234850	2.6	COL3A1	collagen, type iii, alpha-1
Mm.205021	2.4	NPNT	nephronectin
Mm.5020	2.4	SEMA3A	semaphorin 3a
Mm.738	2.1	COL4A1	collagen, type iv, alpha-1
Transcription/translation			
Mm.5025	3.8	ETV4	ets variant gene 4
Mm.9845	3.5	RPS27	ribosomal protein s27
Mm.479	2.9	MYBL1	v-myb myeloblastosis oncogene homolog-like 1
Mm.18810	2.8	ZFP422	zinc finger protein 422
Mm.45039	2.1	LRRFIP1	leucine-rich repeat in flii-interacting protein 1
Mm.925	2.0	TFDP1	transcription factor dp1
Others			
Mm.246318	2.5	EIG180	ethanol-inducble gene 180
Mm.62886	2.0	GALNT7	udp-n-acetyl-a-d-galactosamine:polypeptide n
Mm.29357	14.3	1300017C10RIK	acetylgalacto saminyltransferase 7
Mm.29690	3.0	4930415K17RIK	
Mm.25307	2.3	2810470D21RIK	
Mm.259140	2.2	A230070D14RIK	
Mm.259998	2.2	C730016P09RIK	
Mm.214959	2.2	BB128963	
Mm.38488	2.1	AI256840	

cancer, we performed immunohistochemistry with a multiple tissue array containing 25 pancreatic cancer tissues with defined grade. These pancreatic cancer tissues also showed a stronger CUTL1 protein staining in high histological grade (G2/3) tumors compared to low grade (G1) tumors (see Supplemental Figures S12 and S13). These data on RNA and protein levels strongly indicate that elevated levels of CUTL1 expression may play an important role in enhancing invasiveness and tumor progression in breast and pancreatic cancer.

Discussion

The ability to migrate and invade through the basement membrane into surrounding tissues, blood, and lymphatic vessels is one of the essential hallmarks of cancer and a prerequisite for local tumor progression and metastatic spread. In an RNAi-library-based high-throughput screen for regulators of cell motility (O.E.P. and J.D., unpublished data), we identified CUTL1 as a potential modulator of cell migration. Based on these findings, we examined the role of CUTL1 in the regulation of cell motility and invasiveness. In summary, we found that depletion of CUTL1 from various cell types results in reduction in cell motility and invasiveness, both in vitro and in vivo. CUTL1 is required for the expression of a number of cell surface and other proteins involved in the control of cell adhesion and migration. In addition, TGFβ treatment increases CUTL1 expression, which is required for short-term effects of TGFβ on cell motility. CUTL1 expression is found to correlate with increased histological grade and poor prognosis in breast cancer.

Our hypothesis, based on the RNAi high-throughput screen, that CUTL1 plays a role in the regulation of cell motility could be confirmed experimentally by migration and invasion assays in a number of systems in vitro and in vivo. CUTL1 expression is required for efficient migration of both epithelial and mesenchymal cells on a two-dimensional surface in vitro and for optimal invasion through a three-dimensional gel of extracellular matrix. In addition, reduction in CUTL1 expression severely impaired the ability of tumor cells to form lung colonies in an

Table 2. Genes downregulated by CUTL1

Annotation	Ratio CUTL/RNAi	Gene symbol	Full name
Inflammatory response/chemotaxis			
Mm.26730	0.04	HP	haptoglobin
Mm.465	0.09	CXCL12	chemokine (c-x-c motif) ligand 12
Mm.14277	0.29	SAA3	serum amyloid a 3
Mm.15534	0.36	IL1A	interleukin 1 alpha
Mm.27001	0.48	E430037F08Rik	Riken cdna e430037f08 gene
Extracellular matrix			
Mm.214514	0.01	PRELP	proline arginine-rich repeat/leucine-rich repeat
Mm.22650	0.05	SERPINA3N	serine proteinase inhibitor, clade a, member 3n
Mm.38274	0.06	CHI3L1	chitinase 3-like 1
Mm.18888	0.07	LUM	lumican
Mm.41573	0.09	FMOD	fibromodulin
Mm.102752	0.40	C1GALT1	core 1 udp-gal:acetylgal.-1,3-galactosyltransferase
Mm.18087	0.44	LGALS9	lectin, galactose binding, soluble 9
Others			
Mm.27061	0.16	RIKEN cDNA 0610011I04 GENE	
Mm.28385	0.23	RIKEN cDNA 1810009M01 GENE	

experimental metastasis model in vivo. This assay measures several crucial aspects of the metastatic process, such as the ability of single cancer cells to adhere, survive, and proliferate in a different organ context. Some other prerequisites of metastasis, such as the ability of cells to enter the circulation through a basement membrane, however, are not addressed by the pulmonary colonization assay. Overall, we suggest that high levels of CUTL1 expression are associated with the increased motility typical of invasive carcinoma cells, in contrast to the normally relatively nonmotile untransformed epithelial cells.

Since TGFβ is known to be a major modulator of cell migration and invasion (Massague, 1998; Lehmann et al., 2000), we tested its effect on CUTL1 expression, finding that CUTL1 is transcriptionally induced following TGFβ treatment. We therefore propose that CUTL1 might be a significant new pathway through which TGFβ exerts its promigratory and proinvasive effects. These effects of TGFβ fall into two classes: short-term changes, occurring in a few hours (Seton-Rogers et al., 2004), and long-term changes, requiring altered differentiation of the cell through epithelial-mesenchymal transition (Grunert et al., 2003). CUTL1 does not appear to play a role in the regulation of EMT, but is required for the short-term effects of TGFβ on cell motility, involving both SMAD4-dependent and p38 MAPK-dependent pathways. Initial analysis of the murine CUTL1 promoter suggests the presence of a putative SMAD binding site within 2 kilobases upstream of the transcriptional start site. However, since this site is not consistently conserved among mammalian species, its physiological significance remains to be elucidated. Further investigation will be required to determine the exact mechanism whereby CUTL1 gene expression is controlled by TGFβ.

By using multiple tissue core arrays, we could demonstrate the pathophysiological significance of CUTL1 expression in breast and pancreatic cancer. The increased expression of CUTL1 in high-grade breast and pancreatic cancers and its inverse correlation with overall and relapse-free survival of patients with breast cancer suggests that CUTL1 transcriptional activity has a major impact on tumor progression. The probe used for in situ hybridization will recognize mRNA encoding full-length CUTL1 protein (p200), from which a shorter, more active form (p110) is generated by proteolytic processing. A still shorter version of CUTL1 (p75) is made from an mRNA transcribed from an alternative initiation site within intron 20, but this would not be recognized by the in situ hybridization probe used here (Goulet et al., 2002). CUTL1 p75 has more stable DNA binding activity and has been shown to disrupt tubule formation in collagen by T47D breast carcinoma cells when overexpressed.

Recently, cathepsin cysteine proteases have been described as being important effectors of invasive growth and angiogenesis during multistage tumorigenesis. Several different cathepsins were found to be expressed at increased levels in various cell types involved in tumor progression in the RIP-Tag2 mouse model of pancreatic islet cell carcinogenesis, including cathepsin L, which was expressed exclusively in the tumor cells (Joyce et al., 2004). An isoform of cathepsin L lacking a signal peptide localizes to the nucleus in S phase and has been reported recently to process CUTL1 p200 to the more transcriptionally active p110 form (Goulet et al., 2004). It is possible that increased cathepsin L expression in tumor cells synergizes with elevated CUTL1 levels by promoting its posttranslational processing and activation, leading to elevated expression of CUTL1 target genes involved in tumor cell invasion of surrounding tissue.

We investigated the identity of genes whose expression is regulated by CUTL1 by the combined use of RNA interference technology and microarray expression profiling. Transcriptional profiling after suppression of endogenous CUTL1 expression by shRNA avoids potential biases introduced by overexpression techniques, thus probably providing a more physiologically relevant global expression profile. The gene expression profile observed is likely to be specific for knockdown of CUTL1: we did not observe significant upregulation of interferon-response genes (Bridge et al., 2003), described as nonspecific side effects induced by some siRNAs, and we had no indication of major off-target effects of the RNA sequence used for generating the stable RNAi clones. While these sequences did not have any perfect matches other than CUTL1

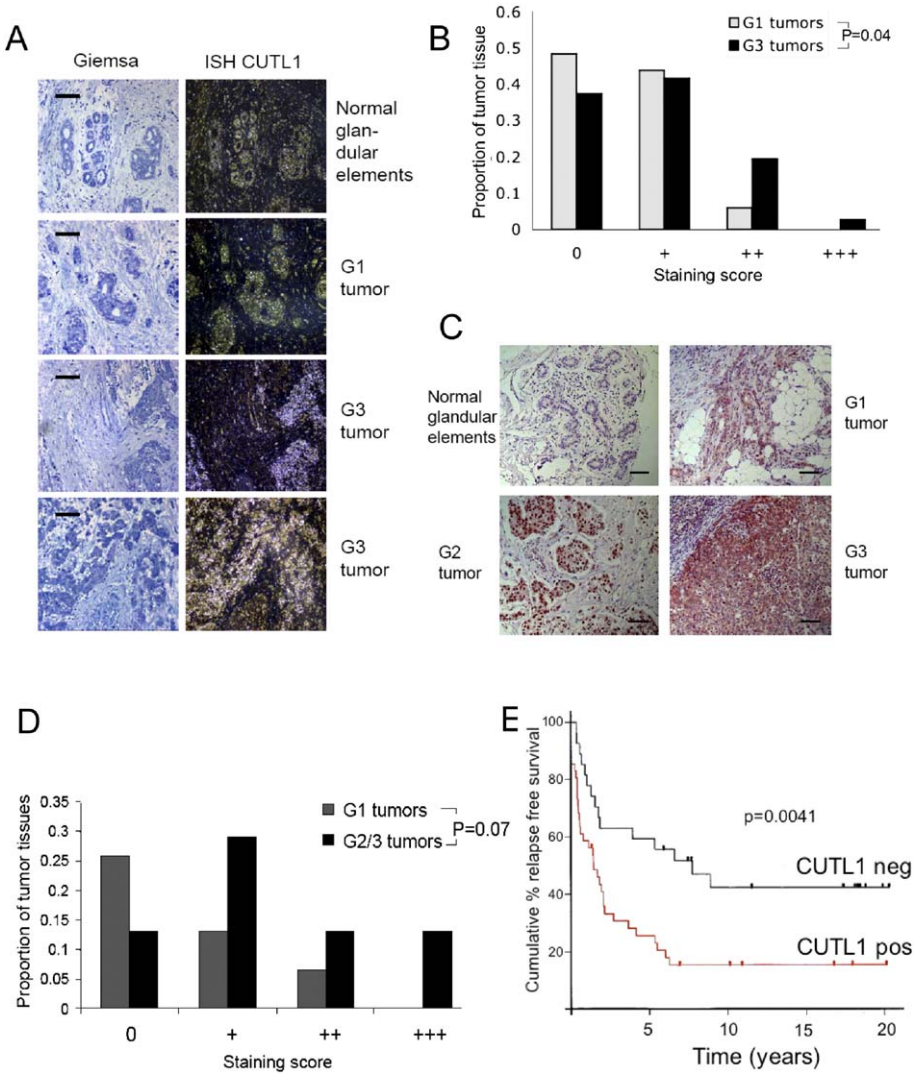

Figure 6. CUTL1 is highly expressed in high-grade breast cancer and correlates with grading and survival

A: In situ hybridization with hCUTL1 probe of 1 normal breast tissue and 3 representative breast cancer tissues with different histopathological grades and increasing levels of CUTL1 RNA. On the right, hCUTL1-positive areas are revealed as autoradiographic silver grains in dark-field images; on the left, the same specimens are shown by Giemsa staining. Bars represent 200 μm.

B: CUTL1 mRNA expression levels in grade 1 (G1) and grade 3 (G3) breast cancers. CUTL1 expression was scored as negative (0), or positive (three levels: +, ++, +++). Proportion of tumors with the respective score out of 138 examined tissues is given. Significance was calculated by nonparametric permutation testing.

C: Immunohistochemistry using the rabbit anti-GST-CUTL antibody of 1 normal breast tissue and 3 representative breast cancer tissues with different histopathological grades and increasing protein levels of CUTL1. Bars represent 100 μm.

D: CUTL1 protein expression levels in grade 1 (G1) and grade 2/3 (G2/3) breast cancers. CUTL1 expression was scored as negative (0) or positive (three levels: +, ++, +++). Proportion of tumors with the respective score out of 35 examined tissues is given. Significance was calculated by nonparametric permutation testing.

E: Inverse association of CUTL1 RNA expression with relapse-free survival in grade 3 ductal breast cancers. Breast tissue carcinomas were grouped as CUTL1-negative or CUTL1-positive, as assessed by ISH, and correlated with the clinical followup of the 68 patients examined. Data are presented as Kaplan-Meier curve and significance was determined using χ^2 testing.

in the relevant mammalian genomes, genes showing partial matches (13–15/19) to the RNAi sequence by BLAST search did not show any suppression of expression in the microarray experiments.

Many of the CUTL1 upregulated target genes identified by the microarray analysis have previously been described as modulators of cell invasion in various tumor cell models: among others, pleiotrophin (PTN), a secreted heparin binding growth factor, induces growth and metastasis in mesenchymal cells (Chauhan et al., 1993) and is rate-limiting for glioblastoma growth (Powers et al., 2002). WNT5A, a member of the wingless gene family, has been associated with motility and invasion of metastatic melanoma (Weeraratna et al., 2002). ALCAM, a member of the immunoglobulin superfamily, enhances growth and migration (van Kempen et al., 2000). S100A10 functions as a plasminogen receptor and has been shown to enhance invasiveness of colorectal cancer cells (Zhang et al., 2004). Perhaps most significantly, α6 integrin (ITGA6) is expressed considerably more strongly in the presence of CUTL1: this integrin, particularly in combination with β4, has been implicated in the progression of several tumor types, including breast cancer (Friedrichs et al., 1995; Guo and Giancotti, 2004). Reduced α6 integrin expression could lead to reduced adhesiveness on laminin extracellular matrix and hence reduced invasiveness. In addition, among the genes negatively regulated by CUTL1 were several proteoglycans, downregulation of which has been associated with poor outcome in invasive breast cancer (Troup et al., 2003).

The data presented here demonstrate that the transcription factor CUTL1 plays a critical role in establishing a pattern of gene expression that favors cancer cell motility and invasive behavior. CUTL1 expression is induced by TGFβ and is required for TGFβ promotion of cell motility. If the technical problems inherent in targeting transcription factors could be overcome, CUTL1 could represent a novel target for the blocking of tumor invasion.

Experimental procedures

Plasmids and siRNA

Myc-tagged full-length human CUTL1 in pMX, as well as CUTL1 nt 831–1336, in pXJ42 were kind gifts from A. Nepveu. The shRNA for mouse and

human CUTL1 (5′-AAGAAGAACACTCCAGAGGATTT-3′) was cloned as hairpin oligonucleotide into pSuper.retro.puro (Oligoengine, Seattle, WA) according to the manufacturer's instructions, and stable clones were obtained after selection with puromycin. The shRNA for mouse SMAD4 was cloned into pSuper (A.R.R., unpublished data) and cotransfected with pBabe.puro for puromycin selection. Control clones were obtained after transfecting the empty vectors.

The reporter plasmids for WNT5A, DAB2, and PTN were generated by PCR amplification of the 2 kb upstream the transcriptional start site and cloning of the 2 kb DNA fragments into the KpnI/BglII sites of pGL3-Enhancer (Promega, Madison, WI). The DNA polymerase α-pGL3-basic-Luc (–1517/+45) was a kind gift from A. Nepveu (Truscott et al., 2003), and the CD34 454-SCL-pXSH-Luc construct was a kind gift from D. Krause (Krause et al., 1997).

For transient transfection of CUTL1 siRNA, the following sense sequences were used (purchased from Ambion, Austin, TX): hCUTL1/I 5′-GGAACAGAAGUUACAGAAUtt-3′, hCUTL1/II 5′-GGAAGCUGAAGCAGCUUUCtt-3′, mCUTL1: 5′-GGUUCUGGAAUAACUCUUUtt-3′. For transient transfection of hSMAD4 siRNA, the following sense sequence was used: hSMAD4 5′-GGUGGAGAGAGUGAAACAUtt-3′. 140 pmole siRNA/well was transfected using Effectene or Transmessenger (Qiagen, Hilden, Germany) as transfection agent in 6-well plates. As negative control, the Silencer Negative Control siRNA from Ambion was used. In the motility assays, cells were transfected with siRNA twice, with an interval of 24 hr. Three hours after the second transfection, the cells were split sparsely for migration, and another three hours later, the tracking experiment was started for 24 hr.

Materials and cell lines

Puromycin (2.5 μg/ml) was obtained from Sigma. The p38MAPK inhibitor SB202190 (10 μM) was from Calbiochem, and rhTGFβ (10 ng/ml) was from R&D systems. ALK4/5/7 inhibitor SB431542 was a kind gift from C. Hill, London. All cell lines were obtained from ATCC.

Multiple tissue core arrays

The human breast carcinoma tissues were obtained from the tissue bank at Cancer Research UK Breast Pathology Laboratory at Guy's Hospital, London. All human tissues were used with approval of the local research ethics committee. Multiple tissue core arrays were produced from representative tumor areas from donor blocks of cases from the Guy's unit and validated as described for in situ hybridization (Gillett et al., 2000). Each case had been previously assessed for tumor size, lymph node status, estrogen, and progesterone receptor status. For detailed characteristics of the cases used see, Supplemental Table S1. Grading was determined by using the modified Bloom & Richardson system (Elston and Ellis, 1991). As independent data sets for immunohistochemical studies, commercially available breast and pancreatic cancer tissue core arrays (Petagen Inc., Seoul, Korea) were used. The breast array contained 4 nonneoplastic breast tissues and 50 carcinoma tissues, among them 35 with defined histological grade (Bloom & Richardson system). The pancreatic array contained 4 nonneoplastic pancreas tissues and 33 carcinoma tissues, among them 25 with defined histological grade which were used for the correlation with CUTL expression. The statistical analyses were calculated using the statistical package S-Plus.

Flow cytometry

FACS analysis was performed as described previously (Michl et al., 2003). For fluorescein diacetate staining (Elliott et al., 2003), cells were resuspended in 1 ml PBS at 10^6 per ml, and 10 μl of fluorescein diacetate (1 μg/ml) was added to the cells for 10 min. For FITC staining (Crissman and Steinkamp, 1973), cells were resuspended in 1 ml PBS containing 5 μl FITC (1 μg/ml), 20 μl propidium iodide (2 mg/ml), and 50 μl RNase (100 μg/ml) for 30 min.

Microarray analysis

Experiments using Affymetrix GeneChip Mouse Genome 430A 2.0 Array oligonucleotide arrays were performed following the manufacturer's recommendation (http://www.affymetrix.com/support/technical/manual/expression_manual.affx). A complete description of all procedures and statistical analysis is available in the MIAME checklist file in the Supplemental Data. Annotation and classification of the genes was performed using MAPPFinder (http://www.genmapp.org/MAPPFinder.html). Significantly regulated genes are presented with the ratio between the mean expression values of two CUTL1 expressing clones and two CUTL1 shRNA knockdown clones each in duplicate experiments (4 data points per group).

RT-PCR

Reverse transcription was performed using the Superscript first strand synthesis kit (Invitrogen). PCR was performed for 30 cycles. Quantitative real-time PCR analyses using the comparative C_T method were performed on an ABI PRISM 7700 Sequence Detector System using the SYBR Green PCR Master Mix kit (Perkin Elmer, Applied Biosystems, Wellesley, MA, USA) according to the manufacturer's instructions. Following initial incubation at 50°C for 2 min and 10 min at 95°C, amplification was performed for 40 cycles at 95°C for 15 s and 60°C for 1 min. Specific primer pairs were determined with the PrimerExpress program (Applied Biosystems). The human cyclophilin A gene (RefSeq ID NM_021130) was used as the internal standard. Primer sequences are available on request.

Western blotting

5×10^5 cells were lysed in HEPES buffer containing 1% Triton X-100, sonicated, size-fractionated by SDS-PAGE on precast gels (NuPAGE, Invitrogen), and blotted onto PVDF membranes (Millipore, Watford, UK). The following antibodies were used for immunodetection: rabbit anti-CDP (Santa Cruz, Santa Cruz, CA), our own rabbit anti-CUTL1 (antigen: GST-hCUTL1 nt2551-3451), goat anti-actin (Santa Cruz), rabbit anti-DAB2 (Santa Cruz), mouse anti-N-cadherin (Zymed, San Francisco, CA), rabbit anti-lumican (kind gift of T. Ishiwata, Tokyo), mouse anti-ALCAM (Antigenix America, Huntington Station, NY), rabbit anti-mouse SDF1A/CXCL12 (Peprotech, London, UK), mouse Annexin II light chain/S100A10 (BD Transduction Laboratories), goat anti-SEMA3A (Santa Cruz), rabbit anti-IL1A (Abcam). Following peroxidase-coupled secondary antiserum (Amersham Pharmacia, Little Chalfont, UK), blots were detected by ECL chemiluminescence (Amersham).

Luciferase reporter assays

Cells were transiently transfected using GeneJuice (Merck Biosciences, Nottingham, UK) according to the manufacturer's instructions, and harvested 24 hr after transfection. Because the internal control plasmid is itself often repressed by CDP/Cux, as a control for transfection efficiency, the purified β-galactosidase protein (Sigma) was included in the transfection mix, as previously described (Truscott et al., 2003; Howcroft et al., 1997). The luciferase assays were performed using the Luciferase Assay System (Promega, Madison, WI), and β-galactosidase activity was detected using 2-Nitrophenyl β-D-galactopyranoside (ONPG, Sigma, Poole, UK) in substrate buffer (1 mM $MgCl_2$, 1 mg/ml ONPG, 75 mM sodium phosphate buffer [pH 7.4], 60 mM β-mercaptoethanol) at 420 nm.

Wound healing assays

An artificial "wound" was created using a 10 μl pipette tip on confluent cell monolayers in 6-well culture plates in serum-containing medium. Photographs were taken at 0 and 8 hr. Quantitative analysis of the wound closure was calculated by counting the number of cells per 10^5 μm^2 wound area at 8 hr.

Two-chamber migration and invasion assays

Cell invasion was determined by using the modified two-chamber migration assay (8 μm pore size, BD Biosciences) or invasion assay (membrane coated with a layer of Matrigel extracellular matrix proteins) according to the manufacturer's instructions. 2.5×10^4 cells were seeded in serum-free medium into the upper chamber and migrated/invaded toward 10% FCS as a chemoattractant in the lower chamber for 6 hr (HT1080 cells) or 18 hr (all other cell lines). Cells in the upper chamber were carefully removed using cotton buds and cells at the bottom of the membrane were fixed and stained with crystal violet 0.2%/methanol 20%. Quantification was performed by counting the stained cells.

Video time-lapse microscopy

Time-lapse imaging of migrating cells was performed on an inverted Zeiss Axiovert 135TV microscope (X-Y-Z motorized stage/piezo Z control; Zeiss,

Jena, Germany) over 24 hr in serum-containing medium at 37°C/10% CO_2. Images were obtained with a Hamamatsu Orca ER firewire CCD camera every 7 or 20 min, and analyzed using image analysis software (AQM Advance6 and Tracker, Kinetic Imaging Ltd, Bromborough, UK). Migration of each cell was analyzed by measuring the distance traveled by a cell nucleus over the 24 hr time period. Statistical analysis was performed using the Mathematica 4.2 software (Wolfram Research, Long Hanborough, UK). The average migration speed in μm/min was calculated by analyzing at least 24 cells/group.

MTT proliferation assay

The cell proliferation kit (MTT, Roche Diagnostics, Mannheim, Germany) was performed in 96-well format according to the manufacturer's instructions.

In vivo metastasis assay

Female NMRI nu/nu mice were injected with 10^6 HT1080, MDA-MB-436, or PANC1 cells/0.1 ml PBS into the tail vein. 6 mice per group were injected, and 2 clones each of cells stably transfected with CUTL shRNA/pRetrosuper or pRetrosuper vector only were used. 17 (HT1080) or 40 (PANC1, MDA-MB-436) days after injection, mice were sacrificed and serial sections of the lungs, cut at a distance of 150 μm from each other, were H&E stained. The number of pulmonary colonies was counted in 15 sections per lung.

In situ hybridization

CUTL1 mRNA levels were studied using in situ hybridization (ISH) as described previously (Poulsom et al., 1998). The human CUTL1 probe (nt 330–1040) was PCR-amplified and cloned into the KpnI and SphI sites of the pGEM3Z vector (Promega). Expression within the tumor epithelium was scored independently in a blinded manner as negative, weak, moderate, or strong. The surrounding tissue stroma showed weak expression of CUTL1. B-actin mRNA was detected on a near serial section as a positive control for each tissue section.

Immunocytochemistry and immunohistochemistry

Cells grown on a coverslip were fixed in 3% paraformaldehyde, incubated with 0.1% Triton X-100, microwaved for antigen retrieval, blocked with 1% BSA, and stained with rabbit anti-CDP (Santa Cruz). As secondary antibody, biotin- or TRITC-labeled anti-rabbit IgG was used. For actin cytoskeleton staining, cells were incubated with Alexa488-conjugated phalloidin (Molecular Probes) according to the manufacturer's protocol. For vinculin staining, a mouse vinculin antibody (Sigma) was used and detected by Cy3-labeled anti mouse-IgG (Dianova, Hamburg). Analysis was performed using a laser scanning confocal microscope (Zeiss Axioplan 2 Upright). Immunohistochemical analysis was performed as previously described (Wagner et al., 2003). In short, paraffin sections were stained after antigen retrieval (microwave in antigen unmasking solution, Vector Laboratories, Burlingame, CA) with rabbit anti-GST-CUTL1 (1:200). Antibody binding was visualized using a biotinylated secondary antibody, avidine conjugated peroxidase (ABC method; Vector Laboratories), and 3,3′diaminobenzidine tetrachloride (DAB) as a substrate, and hematoxylin as counterstain.

Supplemental data

Supplemental data for this article can be found at http://www.cancercell.org/cgi/content/full/7/6/521/DC1/.

Acknowledgments

We thank Dr. A. Nepveu, Dr. D. Krause, and Dr. T. Ishiwata for providing various expression and luciferase constructs, and Dr. Colin Gray, Dr. Daniel Zicha, Dr. Peter Jordan, Deborah Aubyn, Rosemary Jeffery, Toby Hunt, Yvonne Hey, and George Elia for expert technical advice and assistance. Furthermore, we thank Dr. Almut Schulze and Dr. Barbara Nicke for helpful discussions during the preparation of this manuscript, and Gavin Kelly for the statistical analysis. This work was supported by core funding from Cancer Research UK and by a research fellowship from the Deutsche Forschungsgemeinschaft (DFG) to P.M.

Received: November 18, 2004
Revised: April 20, 2005
Accepted: May 24, 2005
Published: June 13, 2005

References

Berns, K., Hijmans, E.M., Mullenders, J., Brummelkamp, T.R., Velds, A., Heimerikx, M., Kerkhoven, R.M., Madiredjo, M., Nijkamp, W., Weigelt, B., et al. (2004). A large-scale RNAi screen in human cells identifies new components of the p53 pathway. Nature *428*, 431–437.

Bridge, A.J., Pebernard, S., Ducraux, A., Nicoulaz, A.L., and Iggo, R. (2003). Induction of an interferon response by RNAi vectors in mammalian cells. Nat. Genet. *34*, 263–264.

Chauhan, A.K., Li, Y.S., and Deuel, T.F. (1993). Pleiotrophin transforms NIH 3T3 cells and induces tumors in nude mice. Proc. Natl. Acad. Sci. USA *90*, 679–682.

Coqueret, O., Berube, G., and Nepveu, A. (1996). DNA binding by cut homeodomain proteins is down-modulated by protein kinase C. J. Biol. Chem. *271*, 24862–24868.

Coqueret, O., Berube, G., and Nepveu, A. (1998). The mammalian Cut homeodomain protein functions as a cell-cycle-dependent transcriptional repressor which downmodulates p21WAF1/CIP1/SDI1 in S phase. EMBO J. *17*, 4680–4694.

Crissman, H.A., and Steinkamp, J.A. (1973). Rapid, simultaneous measurement of DNA, protein, and cell volume in single cells from large mammalian cell populations. J. Cell Biol. *59*, 766–771.

Elliott, J.T., Tona, A., and Plant, A.L. (2003). Comparison of reagents for shape analysis of fixed cells by automated fluorescence microscopy. Cytometry *52A*, 90–100.

Ellis, T., Gambardella, L., Horcher, M., Tschanz, S., Capol, J., Bertram, P., Jochum, W., Barrandon, Y., and Busslinger, M. (2001). The transcriptional repressor CDP (Cutl1) is essential for epithelial cell differentiation of the lung and the hair follicle. Genes Dev. *15*, 2307–2319.

Elston, C.W., and Ellis, I.O. (1991). Pathological prognostic factors in breast cancer. I. The value of histological grade in breast cancer: Experience from a large study with long-term follow-up. Histopathology *19*, 403–410.

Friedrichs, K., Ruiz, P., Franke, F., Gille, I., Terpe, H.J., and Imhof, B.A. (1995). High expression level of α6 integrin in human breast carcinoma is correlated with reduced survival. Cancer Res. *55*, 901–906.

Gillett, C.E., Springall, R.J., Barnes, D.M., and Hanby, A.M. (2000). Multiple tissue core arrays in histopathology research: A validation study. J. Pathol. *192*, 549–553.

Goulet, B., Watson, P., Poirier, M., Leduy, L., Berube, G., Meterissian, S., Jolicoeur, P., and Nepveu, A. (2002). Characterization of a tissue-specific CDP/Cux isoform, p75, activated in breast tumor cells. Cancer Res. *62*, 6625–6633.

Goulet, B., Baruch, A., Moon, N.S., Poirier, M., Sansregret, L.L., Erickson, A., Bogyo, M., and Nepveu, A. (2004). A cathepsin L isoform that is devoid of a signal peptide localizes to the nucleus in S phase and processes the CDP/Cux transcription factor. Mol. Cell *14*, 207–219.

Guo, W., and Giancotti, F.G. (2004). Integrin signalling during tumour progression. Nat. Rev. Mol. Cell Biol. *5*, 816–826.

Grunert, S., Jechlinger, M., and Beug, H. (2003). Diverse cellular and molecular mechanisms contribute to epithelial plasticity and metastasis. Nat. Rev. Mol. Cell Biol. *4*, 657–665.

Harada, R., Berube, G., Tamplin, O.J., Denis-Larose, C., and Nepveu, A.

(1995). DNA-binding specificity of the cut repeats from the human cut-like protein. Mol. Cell. Biol. *15*, 129–140.

Howcroft, T.K., Kirshner, S.L., and Singer, D.S. (1997). Measure of transient transfection efficiency using beta-galactosidase protein. Anal. Biochem. *244*, 22–27.

Inman, G.J., Nicolas, F.J., Callahan, J.F., Harling, J.D., Gaster, L.M., Reith, A.D., Laping, N.J., and Hill, C.S. (2002). SB-431542 is a potent and specific inhibitor of transforming growth factor-beta superfamily type I activin receptor-like kinase (ALK) receptors ALK4, ALK5, and ALK7. Mol. Pharmacol. *62*, 65–74.

Jechlinger, M., Grunert, S., Tamir, I.H., Janda, E., Ludemann, S., Waerner, T., Seither, P., Weith, A., Beug, H., and Kraut, N. (2003). Expression profiling of epithelial plasticity in tumor progression. Oncogene *22*, 7155–7169.

Joyce, J.A., Baruch, A., Chehade, K., Meyer-Morse, N., Giraudo, E., Tsai, F.Y., Greenbaum, D.C., Hager, J.H., Bogyo, M., and Hanahan, D. (2004). Cathepsin cysteine proteases are effectors of invasive growth and angiogenesis during multistage tumorigenesis. Cancer Cell *5*, 443–453.

Krause, D.S., Kapadia, S.U., Raj, N.B., and May, W.S. (1997). Regulation of CD34 expression in differentiating M1 cells. Exp. Hematol. *25*, 1051–1061.

Ledford, A.W., Brantley, J.G., Kemeny, G., Foreman, T.L., Quaggin, S.E., Igarashi, P., Oberhaus, S.M., Rodova, M., Calvet, J.P., and Vanden Heuvel, G.B. (2002). Deregulated expression of the homeobox gene Cux-1 in transgenic mice results in downregulation of p27(kip1) expression during nephrogenesis, glomerular abnormalities, and multiorgan hyperplasia. Dev. Biol. *245*, 157–171.

Lehmann, K., Janda, E., Pierreux, C.E., Rytomaa, M., Schulze, A., McMahon, M., Hill, C.S., Beug, H., and Downward, J. (2000). Raf induces TGFbeta production while blocking its apoptotic but not invasive responses: A mechanism leading to increased malignancy in epithelial cells. Genes Dev. *14*, 2610–2622.

Luong, M.X., van der Meijden, C.M., Xing, D., Hesselton, R., Monuki, E.S., Jones, S.N., Lian, J.B., Stein, J.L., Stein, G.S., Neufeld, E.J., and Van Wijnen, A.J. (2002). Genetic ablation of the CDP/Cux protein C terminus results in hair cycle defects and reduced male fertility. Mol. Cell. Biol. *22*, 1424–1437.

Massague, J. (1998). TGF-beta signal transduction. Annu. Rev. Biochem. *67*, 753–791.

Micchelli, C.A., Rulifson, E.J., and Blair, S.S. (1997). The function and regulation of cut expression on the wing margin of Drosophila: Notch, Wingless and a dominant negative role for Delta and Serrate. Development *124*, 1485–1495.

Michl, P., Barth, C., Buchholz, M., Lerch, M.M., Rolke, M., Holzmann, K.H., Menke, A., Fensterer, H., Giehl, K., Lohr, M., et al. (2003). Claudin-4 expression decreases invasiveness and metastatic potential of pancreatic cancer. Cancer Res. *63*, 6265–6271.

Nepveu, A. (2001). Role of the multifunctional CDP/Cut/Cux homeodomain transcription factor in regulating differentiation, cell growth and development. Gene *270*, 1–15.

Poulsom, R., Longcroft, J.M., Jeffery, R.E., Rogers, L.A., and Steel, J.H. (1998). A robust method for isotopic riboprobe in situ hybridisation to localise mRNAs in routine pathology specimens. Eur. J. Histochem. *42*, 121–132.

Powers, C., Aigner, A., Stoica, G.E., McDonnell, K., and Wellstein, A. (2002). Pleiotrophin signaling through anaplastic lymphoma kinase is rate-limiting for glioblastoma growth. J. Biol. Chem. *277*, 14153–14158.

Santaguida, M., Ding, Q., Berube, G., Truscott, M., Whyte, P., and Nepveu, A. (2001). Phosphorylation of the CCAAT displacement protein (CDP)/Cux transcription factor by cyclin A-Cdk1 modulates its DNA binding activity in G(2). J. Biol. Chem. *276*, 45780–45790.

Seton-Rogers, S.E., Lu, Y., Hines, L.M., Koundinya, M., LaBaer, J., Muthuswamy, S.K., and Brugge, J.S. (2004). Cooperation of the ErbB2 receptor and transforming growth factor beta in induction of migration and invasion in mammary epithelial cells. Proc. Natl. Acad. Sci. USA *101*, 1257–1262.

Sinclair, A.M., Lee, J.A., Goldstein, A., Xing, D., Liu, S., Ju, R., Tucker, P.W., Neufeld, E.J., and Scheuermann, R.H. (2001). Lymphoid apoptosis and myeloid hyperplasia in CCAAT displacement protein mutant mice. Blood *98*, 3658–3667.

Skalnik, D.G., Strauss, E.C., and Orkin, S.H. (1991). CCAAT displacement protein as a repressor of the myelomonocytic-specific gp91-phox gene promoter. J. Biol. Chem. *266*, 16736–16744.

Tavares, A.T., Tsukui, T., and Izpisua Belmonte, J.C. (2000). Evidence that members of the Cut/Cux/CDP family may be involved in AER positioning and polarizing activity during chick limb development. Development *127*, 5133–5144.

Troup, S., Njue, C., Kliewer, E.V., Parisien, M., Roskelley, C., Chakravarti, S., Roughley, P.J., Murphy, L.C., and Watson, P.H. (2003). Reduced expression of the small leucine-rich proteoglycans, lumican, and decorin is associated with poor outcome in node-negative invasive breast cancer. Clin. Cancer Res. *9*, 207–214.

Truscott, M., Raynal, L., Premdas, P., Goulet, B., Leduy, L., Berube, G., and Nepveu, A. (2003). CDP/Cux stimulates transcription from the DNA polymerase alpha gene promoter. Mol. Cell. Biol. *23*, 3013–3028.

van Gurp, M.F., Pratap, J., Luong, M., Javed, A., Hoffmann, H., Giordano, A., Stein, J.L., Neufeld, E.J., Lian, J.B., Stein, G.S., and Van Wijnen, A.J. (1999). The CCAAT displacement protein/cut homeodomain protein represses osteocalcin gene transcription and forms complexes with the retinoblastoma protein-related protein p107 and cyclin A. Cancer Res. *59*, 5980–5988.

van Kempen, L.C., van den Oord, J.J., van Muijen, G.N., Weidle, U.H., Bloemers, H.P., and Swart, G.W. (2000). Activated leukocyte cell adhesion molecule/CD166, a marker of tumor progression in primary malignant melanoma of the skin. Am. J. Pathol. *156*, 769–774.

Van Wijnen, A.J., van Gurp, M.F., de Ridder, M.C., Tufarelli, C., Last, T.J., Birnbaum, M., Vaughan, P.S., Giordano, A., Krek, W., Neufeld, E.J., et al. (1996). CDP/cut is the DNA-binding subunit of histone gene transcription factor HiNF-D: A mechanism for gene regulation at the G1/S phase cell cycle transition point independent of transcription factor E2F. Proc. Natl. Acad. Sci. USA *93*, 11516–11521.

Wagner, M., Kunsch, S., Duerschmied, D., Beil, M., Adler, G., Mueller, F., and Gress, T.M. (2003). Transgenic overexpression of the oncofetal RNA binding protein KOC leads to remodeling of the exocrine pancreas. Gastroenterology *124*, 1901–1914.

Weeraratna, A.T., Jiang, Y., Hostetter, G., Rosenblatt, K., Duray, P., Bittner, M., and Trent, J.M. (2002). Wnt5a signaling directly affects cell motility and invasion of metastatic melanoma. Cancer Cell *1*, 279–288.

Yu, L., Hebert, M.C., and Zhang, Y.E. (2002). TGF-beta receptor-activated p38 MAP kinase mediates Smad-independent TGF-beta responses. EMBO J. *21*, 3749–3759.

Zeng, W.R., Watson, P., Lin, J., Jothy, S., Lidereau, R., Park, M., and Nepveu, A. (1999). Refined mapping of the region of loss of heterozygosity on the long arm of chromosome 7 in human breast cancer defines the location of a second tumor suppressor gene at 7q22 in the region of the CUTL1 gene. Oncogene *18*, 2015–2021.

Zhang, L., Fogg, D.K., and Waisman, D.M. (2004). RNA interference-mediated silencing of the S100A10 gene attenuates plasmin generation and invasiveness of Colo 222 colorectal cancer cells. J. Biol. Chem. *279*, 2053–2062.